



SNRPB promotes cervical cancer progression through repressing p53 expression

Zhu Lei^{a,1}, Zhang Xiuzhen^{b,1}, Sun Ziqin^{c,*}

^a Department of Gynecology and Obstetrics, Beijing Chaoyang Hospital Affiliated Capital Medical University, Beijing, 100020, China

^b Department of 1st Department Gynecology Oncology, Shaanxi Provincial Tumor Hospital, Xi'an, Shaanxi, 710061, China

^c Department of Women's Insurance, Ankang Maternity and Childcare Hospital, West Section of Hanjiang Road, High-tech Zone, Ankang City, Shaanxi Province, 725000, China



ARTICLE INFO

Keywords:

Cervical cancer
SNRPB
Migration and invasion
p53

ABSTRACT

Cervical cancer is still a leading cause of tumor death in women across the world. Small nuclear ribonucleoprotein polypeptides B and B1 (SNRPB) gene encodes the components of the core spliceosomal machinery, and regulates the development of several types of cancers. However, its function in cervical cancer progression remains unclear. In the study, we found that SNRPB was highly expressed in human cervical cancer tissues and in cervical cancer cell lines. Meanwhile, SNRPB knockdown using shRNA in cervical cancer cells markedly reduced the cell proliferation, migration and invasion. Furthermore, the increased percentage of cells in G2/M phase and apoptotic cell death was detected in cervical cancer cells with SNRPB knockdown, suggesting that SNRPB might contribute to cervical cancer growth. Moreover, we found that SNRPB could directly interact with p53, and the interaction showed an essential role in modulating cervical cancer cell proliferation, migration, invasion and apoptosis. In xenograft model, the knockdown of SNRPB exerted effectively anti-cervical cancer ability characterized by the reduced tumor volume and weight, and a remarkable reduction in KI-67 expression. Improved expression of p53 validated the *in vitro* findings. Therefore, SNRPB might be a potent therapeutic target in cervical cancer through interacting with p53.

1. Introduction

Cervical cancer is one of the most common tumors among female in the world, and is a leading cause of cancer death for women especially in the developing countries [1]. Presently, the high-risk human papillomavirus (HPV) infection is pivotal for the progression of cervical cancer. In addition, the genetic changes and epigenetic modifications also play important roles in regulating cervical cancer development [2,3]. Meanwhile, the primary methods for the treatments of cervical cancer include surgery, radiotherapy and adjuvant chemotherapy, which have significantly improved the survival rate of patients with cervical cancer [4,5]. Unfortunately, accumulating studies have showed that excessive radioresistance or chemoresistance, repeated relapse as well as tumor metastasis limit the treatment efficacy, and the molecular mechanisms revealing cervical cancer growth are not fully investigated and understood. Therefore, it is urgently necessary to find novel or critical therapeutic target to develop effective and reliable treatments.

Small nuclear ribonucleoprotein polypeptides B and B1 (SNRPB)

gene is the core component of spliceosomal small nuclear ribonucleoproteins [snRNPS], playing a crucial role in controlling the pre-mRNA splicing [6]. Presently, SNRPB is reported to be the cause of cerebrocosto-mandibular syndrome (CCMS), and shows the strongest influences on the viability, proliferation, and apoptosis [7,8]. Recently, SNRPB expression was detected to be increased in glioblastoma. In brief, suppressing SNRPB expression down-regulated the cell viability and improved cellular apoptosis in glioma cell lines [9]. Furthermore, bioinformatics analysis demonstrated that SNRPB was also involved in the pathogenesis of lung cancer. SNRPB was more recently reported to facilitate the progression of non-small cell lung cancer (NSCLC) mainly through regulating the expression change of RAB26, whose aberrant expression is tightly associated with tumor inhibition or the process of tumorigenesis [10]. Although the oncogenic functions of SNRPB have been reported, its specific function in contributing to cervical cancer is almost unknown.

In the current study, we found the significantly increased expression of SNRPB in tumor samples from patients with cervical cancer, and in

* Corresponding author.

E-mail address: zz191vip@qq.com (Z. Sun).

¹ The first two authors contributed equally to this work.

several cervical cancer cell lines. SNRPB knockdown by shRNA reduced the cervical cancer cell proliferation, migration and invasion *in vitro*, and also suppressed tumor growth *in vivo*. Furthermore, our results identified that SNRPB could interact with p53, playing a major role in mediating cervical cancer development. Collectively, findings here suggested SNRPB as a novel regulator in cervical cancer, which thus could be served as an effective target to develop reliable treatments.

2. Materials and methods

2.1. Cell culture

Human cervical cancer cell lines (CaSki, HeLa, SiHa, C33A and HT-3), and human cervical epithelial cells (H8) were purchased from Chinese Type Culture Collection, Chinese Academy of Sciences. All cells were cultured in DMEM (Hyclone, USA) supplemented with 10 % fetal bovine serum (FBS, Hyclone) and 100 U/ml penicillin sodium. All cells were cultured in an incubator with an atmosphere of 5 % CO₂ at 37 °C. Short hairpin RNA (shRNA) that targeted human SNRPB (shSNRPB), human p53 (sh-p53) and GFP (served as shNC) was obtained from Sangon Biotech (Shanghai, China), which were then cloned into the pLKO.1 vector. The pcDNA3.1 vector targeting SNRPB, and its empty vectors were acquired from RIBOBIO (Guangdong, China). Cervical cancer cells were then transfected with plasmids by Lipo3000 Transfection Reagent (Invitrogen, USA) following the manufacturer's protocols. After 24 h of transfection, all cells were collected for subsequent analysis. The p53 activator (Tenovin-6) and inhibitor (PFTα) were purchased from Selleck (USA) and Sigma Aldrich (USA). The recombinant human SNRPB (rhSNRPB) was purchased from Abcam (USA) to rescue SNRPB expression levels in cervical cancer cells.

2.2. RT-qPCR analysis

RNA was isolated using the TRIzol Reagent (Invitrogen, USA) following the manufacturer's instructions. The cDNA was synthesized with random primers using the PrimeScript™ RT Reagent Kit with gDNA Eraser (Takara, Japan) according to manufacturer's protocols. RT-qPCR was carried out using AceQ qPCR SYBR Green Master Mix (Vazyme Biotech, Nanjing, China) on a Chromo4 real-time PCR detection system (Bio-Rad, USA). The PCR primer sequences were shown as followings: GAPDH, forward, 5'-GCA CCG TCA AGG CTG AGA AC-3'; reverse, 5'-TGG TGA AGA CGC CAG TGG A-3'; SNRPB, forward, 5'-CCG GAT CTT CAT TGG CAC CT-3'; reverse, 5'-AGG ACT CGC TTC TCT TCC CT-3'. The relative gene expression was normalized to control by the 2^{-ΔΔCt} method.

2.3. Western blot analysis

Total proteins from cells or tissues were extracted with radio-immunoprecipitation assay (RIPA) lysis buffer (Beyotime, Nanjing, China). Western blot was conducted using specific antibodies against SNRPB (ab155026, Abcam), p53 (ab131442, Abcam), CDK1 (ab133327, Abcam), CDK2 (ab32147, Abcam), N-cadherin (ab18203, Abcam), E-cadherin (ab1416, Abcam), Vimentin (ab92547, Abcam), Snail (ab53519, Abcam), MMP9 (ab38898, Abcam), cleaved Caspase-3 (ab49822, Abcam), cleaved PARP (ab32064, Abcam) and GAPDH (ab181606, Abcam). After incubation with horseradish peroxidase (HRP)-conjugated secondary antibodies (1:5000, Beyotime), the protein bands were detected using chemiluminescence substrate (Pierce, USA) and then exposed to Kodak X-OMATAR autoradiography film (Eastman Kodak, USA).

2.4. Cell proliferation by CCK8

Cell proliferation was measured using Cell counting Kit-8 (CCK8, Dojindo Laboratories, Japan) according to the

manufacturer's protocols. Absorbance was measured at 450 nm using a microplate reader.

2.5. Colony formation

Cells in 6-well plates were incubated in DMEM with 10 % FBS for 2 weeks at 37 °C 5 % CO₂. The cell colonies were rinsed, fixed with 4 % paraformaldehyde and stained with 0.1 % gentian violet solution. The individual clones (> 50 cells) were counted and analyzed.

2.6. Flow cytometry analysis

After treatments, cells were fixed in 70 % cold ethanol overnight at 4 °C. After washing with PBS, the cells were incubated in 0.5 μg/mL of PI and 10 mg/mL of RNase (Sigma Aldrich) at room temperature for 30 min. Next, the samples were calculated using FACS (BD Biosciences, USA).

For the flow cytometric quantification of cell death, the cells were treated as indicated. Then, cells were collected, washed twice with PBS and stained using Annexin VFITC/PI (BD Biosciences) according to the manufacturer's instructions. Stained cells were analyzed using a FACS (BD Biosciences), and data were processed using FlowJo software.

2.7. Migration and invasion

For migration and invasion analysis, cancer cells were resuspended in 200 μl of serum-free medium (Hyclone) and placed in the upper compartment of a Transwell chamber (Corning, USA) with or without matrigel (BD Biosciences). The migrated or invaded cells was fixed and stained with crystal violet. Six random fields were selected for analyzing with a light microscope.

2.8. Tumorsphere-forming efficiency analysis

HeLa and SiHa cells were cultured in stem cell media consisted of DMEM/F12 basal media (Hyclone) N2, and B27 supplements (Invitrogen), 20 ng/mL human recombinant epidermal growth factor, and 20 ng/mL basic fibroblastic growth factor (Sigma Aldrich). For the tumorsphere analysis, cells were cultured in 96-well plates and sustained in stem cell medium. Tumor spheres that arose in 2 weeks were recorded.

2.9. Co-immunoprecipitation (Co-IP), plasmid constructs and GST fusion protein purification and GST pull down assays

The collected cells were lysed in Lysis Buffer for IP (Beyotime). Then, the lysates were incubated with the indicated antibodies overnight at 4 °C on a rocker, followed by immunoprecipitation with Protein A + G Agarose (Beyotime) at 4 °C for 3 h. The immunoprecipitates were analyzed using western blot. Sequences encoding full-length SNRPB and p53 genes were cloned into pcDNA5-Flag and pcDNA5-HA vectors to generate pcDNA5-Flag-SNRPB and pcDNA5-HA-p53, respectively. Plasmids encoding pcDNA5-HA-GST-SNRPB and pcDNA5-HA-GST-p53 were obtained by cloning the indicated cDNA of SNRPB and p53, respectively, into pcDNA5-HA-GST vectors. IP was performed as previously described [11,12]. Briefly, after transient transfection with plasmid, HeLa cells were lysed in ice-cold IP buffer. The cell lysates were incubated with the indicated antibody-conjugated beads (Anti-Flag M2 Magnetic Beads, Sigma; Pierce Anti-HA Magnetic Beads, Thermo Fisher Scientific) at 4 °C overnight. The immune complexes were subjected to immunoblotting using the indicated primary and corresponding secondary antibodies. Rosetta (DE3) *Escherichia coli* were separately transformed with HA-GST-SNRPB- and HA-GST-p53-encoding plasmid and then induced using 0.5 mM isopropyl-β-D-thiogalactopyranoside after the culture reached an optical density of 0.8 at 600 nm (OD600). The isolated proteins were eluted in elution buffer

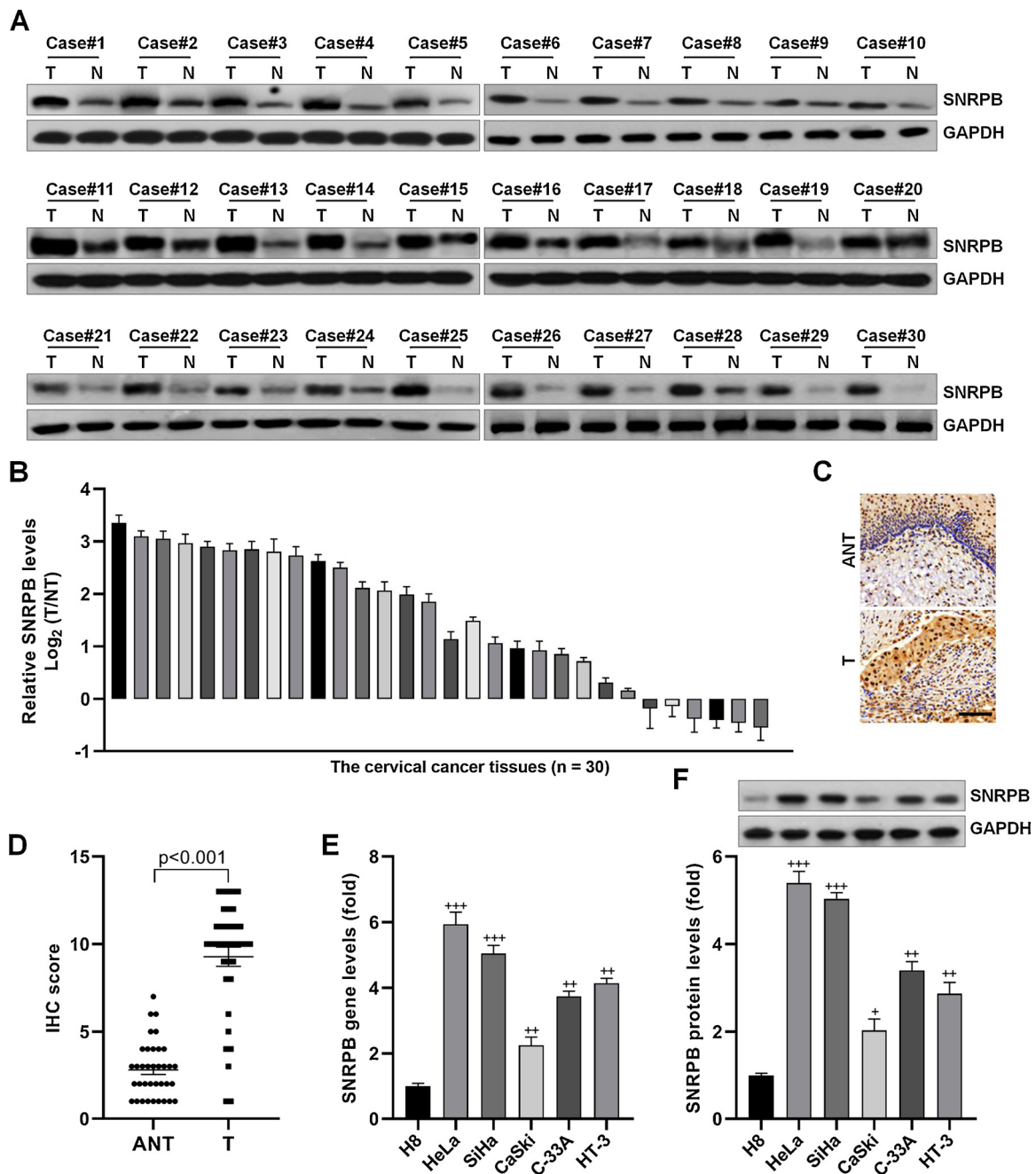


Fig. 1. SNRPB expression was up-regulated in cervical cancer. (A) Western blot for SNRPB protein expression levels in cervical tumor tissues (T) and adjacent non-tumor tissues (N) (n = 30). (B) RT-qPCR for SNRPB mRNA expression levels in cervical tumor tissues and adjacent non-tumor tissues (n = 36). (C) Immunohistochemical analysis of SNRPB in cervical cancer specimens. (D) Quantification of the average score of SNRPB staining between the paired cervical cancer samples and the adjacent non-tumor tissues. SNRPB expression in five cervical cancer cell lines (HeLa, CaSki, C-33A and HT-3) and the normal cell line (H8) by (E) RT-qPCR and (F) western blotting analysis. +P < 0.05, ++P < 0.01 and +++P < 0.001. The data were presented as the mean ± S.E.M.

(50 mM Tris-HCl, pH 8.0; and 20 mM reduced glutathione), resolved via SDS-PAGE and then analyzed with western blotting using the indicated antibodies.

2.10. Tumor xenograft model

The animal study was approved by the Animal Experimentation Ethics Committee of Beijing Chaoyang Hospital Affiliated Capital Medical University (Beijing, China). Female BALB/c nude mice (4 weeks of age) were purchased from Beijing HFK Bioscience (Beijing) and kept in a sterile environment. 5×10^6 of HeLa cells with or without SNRPB knockdown resuspended in 100 μ L of PBS were subcutaneously

injected into the right dorsal region of each animal, respectively. 1 week after implantation, mice were randomly divided into 2 groups (n = 5/group), including shNC and shSNRPB. Tumor volumes were monitored and measured every 2 days by calculating the length (L) and the width (W), and calculated by the volume ($V = L \times W^2/2$). After 28 days, all mice were killed. Tumor samples were exercised, weighed and frozen in liquid nitrogen or fixed in 10 % formalin for further analysis.

2.11. Immunohistochemical analysis

The removed tumors were fixed in formalin, embedded in paraffin, and cut into 5- μ m sections for H&E staining and immunohistochemical

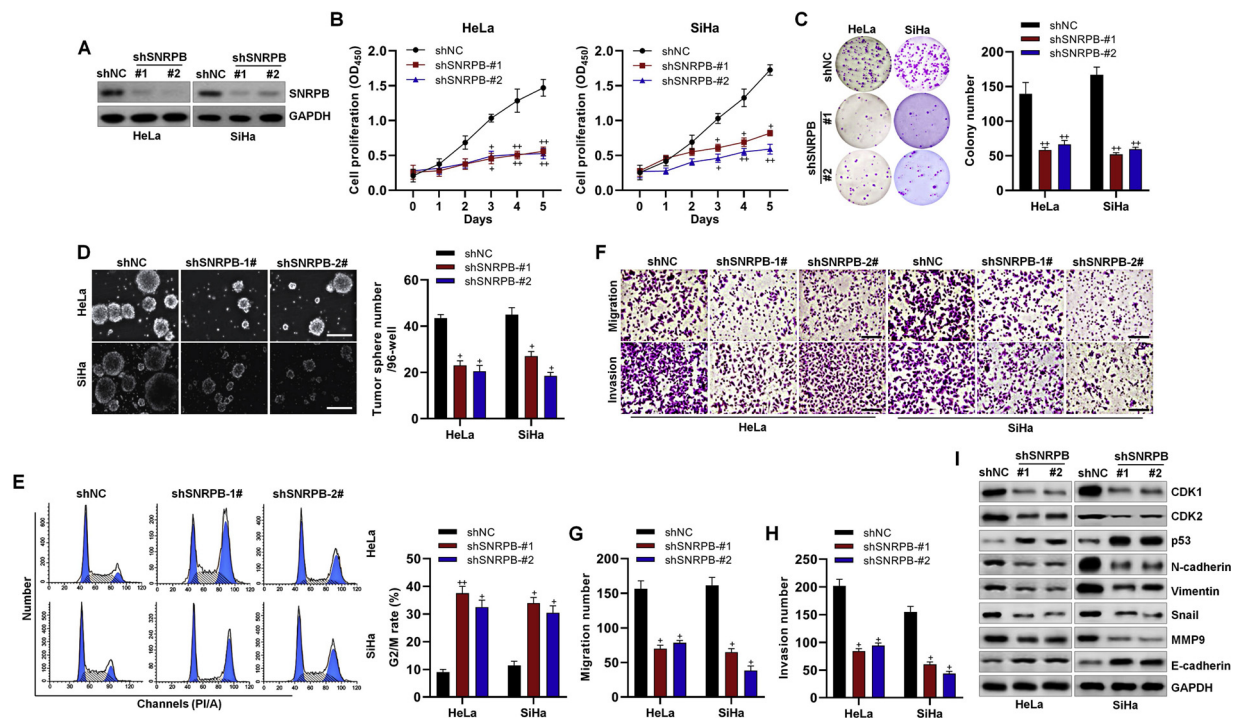


Fig. 2. Suppressing SNRPB inhibited proliferation, migration and invasion in cervical cancer cells. (A) HeLa and SiHa cells were transfected with shSNRPB-1# or shSNRPB-2# sequences for 24 h, and shNC was served as a control. Western blot analysis was used to calculate the efficiency. (B) CCK8 and (C) colony formation assays were performed to determine the cell proliferation in cervical cancer cells with SNRPB knockdown. (D) Tumor sphere-forming efficiency analysis in HeLa and SiHa cells after SNRPB knockdown. (E) Flow cytometry analysis for cell cycle calculation in cervical cancer cells after SNRPB knockdown. Quantification (%) of cells in G2/M was exhibited. (F) The migration and invasion of cervical cancer cells were determined after SNRPB knockdown. Quantification of the number of cells in (G) migration and (H) invasion. (I) Western blot analysis was performed to evaluate the protein expression levels of signals associated with cell cycle regulation (CDK1, CDK2 and p53) and metastasis (N-cadherin, Vimentin, Snail, MMP9 and E-cadherin) in cervical cancer cells after SNRPB knockdown. The data were presented as the mean \pm S.E.M. $^+P < 0.05$ and $^{++}P < 0.01$ compared to the shNC group.

analysis as previously described [13]. The tumor sections were stained using antibodies against p53 (ab131442), KI-67 (ab15580), CDK1 (ab133327), E-cadherin (ab1416), N-cadherin (ab18203) (all antibodies mentioned above were purchased from Abcam), cleaved Caspase-3 (PA5-36746, Thermo Fisher Scientific) and SNRPB (MA5-13449, Invitrogen). In brief, formalin fixed tumor tissues (5 μ m thickness) were dewaxed, rehydrated, and then incubated in 3 % H_2O_2 to quench the endogenous peroxidase activity. After antigen retrieval with citrate buffer, the sections were incubated with normal rabbit serum (Solarbio, Beijing, China) at 37 $^{\circ}C$ for 30 min, followed by incubation with the shown primary antibodies. Then, all slides were reacted with diaminobenzidine (DAB, Beyotime) and counterstained with Mayer hematoxylin (Beyotime). TUNEL Assay Kit-HRP-DAB (ab206386, Abcam) was used for apoptosis analysis in tumor samples according to the manufacturer's instructions. Representative images were obtained under a microscope.

2.12. Immunofluorescence

Cells were fixed with 4 % paraformaldehyde, permeabilized with 0.05 % TritonX 100, and blocked with 10 % donkey serum (Sigma Aldrich). After incubating with primary antibodies overnight including SNRPB (1:100, Abcam) and p53 (1:150, Abcam), secondary fluorescent antibodies (Solarbio, Beijing, China) were added to cells. DAPI (Sigma Aldrich) was used for nuclear staining. Samples were observed with a confocal microscope.

2.13. Patient specimens

Surgical resection of 36 tumor tissue samples and the matched adjacent normal cervix fresh tissues from patients with primary cervical

cancer were obtained from the Beijing Chaoyang Hospital Affiliated Capital Medical University between January 2009 and December 2017, and were used for immunohistochemistry analysis. No patients had once received radiotherapy or chemotherapy before surgery. The histology of all cervical cancer tissues was verified by surgical pathologists. Then, the histological subtype and stage of the tumor samples were categorized according to the International Federation of Gynecology and Obstetrics (FIGO) classification. The experimental protocols for the human study were approved by the Research Ethics Board in Beijing Chaoyang Hospital Affiliated Capital Medical University, and informed consent was obtained from all patients included.

2.14. Statistical analysis

All data were reported as mean \pm S.E.M. All analysis was conducted using Prism 8.0 (Graph-Pad Software, USA). Differences between groups were calculated with Student's *t*-test. Comparisons where *p* values < 0.05 were served significant.

3. Results

3.1. SNRPB expression was up-regulated in cervical cancer

To investigate the effects of SNRPB on cervical cancer progression, we first explored its expression change in tumor tissues from patients with cervical cancer. As shown in Fig. 1A, western blot analysis demonstrated that SNRPB expression was up-regulated in cervical tumor samples compared to that of the adjacent normal cervix tissues. RT-qPCR analysis confirmed that cervical cancer samples showed higher expression levels of SNRPB (Fig. 1B). Immunohistochemistry

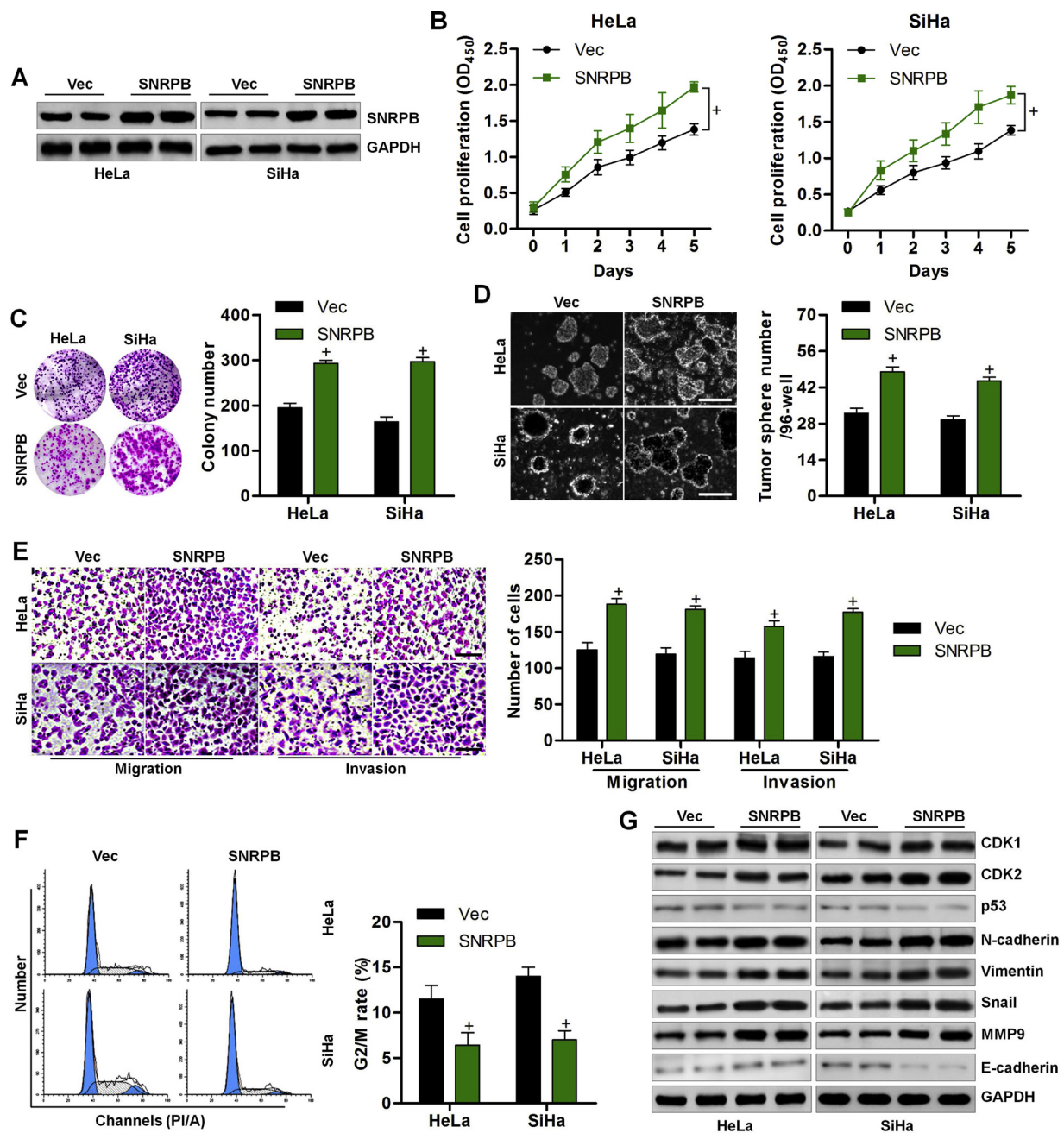


Fig. 3. SNRBP over-expression accelerated the proliferation, migration and invasion in cervical cancer cells. HeLa and SiHa cells were transfected with pcDNA3.1-SNRBP for 24 h. Then, all cells were harvested for the following studies. (A) The interference efficiency calculation using western blotting analysis. (B) CCK8 analysis was used to calculate the cell proliferation. (C) Colony formation analysis. (D) Tumor sphere-forming efficiency analysis in HeLa and SiHa cells with SNRBP over-expression. (E) Transwell analysis was used for the determination of migration and invasion. (F) Flow cytometry analysis for the calculation of cells distributed in G2/M. (G) Western blotting analysis of CDK1, CDK2, p53, N-cadherin, Vimentin, Snail, MMP9 and E-cadherin. The data were presented as the mean \pm S.E.M. $^+P < 0.05$ and $^{++}P < 0.01$ compared to the shNC group.

demonstrated that the expression of SNRBP tended to be lower in cervical tumor samples than adjacent normal tissues (Fig. 1C and D). *In vitro* analysis further indicated that SNRBP mRNA and protein expression levels were markedly increased in cervical cancer cell lines when compared to that of the human cervical epithelial cells (H8) (Fig. 1E and F). As shown in Supplementary Fig. 1A and B, both RT-qPCR and western blotting results demonstrated that SNRBP mRNA and protein expression levels were higher in gastric cancer cells, lung cancer cells and breast cancer cells when compared with the corresponding non-tumor cells. However, no significant difference was detected in the prostate cancer cells. These findings demonstrated that SNRBP up-regulation might be associated with cervical cancer progression in a

positive manner.

3.2. Suppressing SNRBP inhibited proliferation, migration and invasion in cervical cancer cells

Human cervical cancer cell lines HeLa and SiHa were then infected with lentiviruses with shSNRBP-#1 or shSNRBP-#2 to produce stable cell lines with SNRBP knockdown (Fig. 2A). CCK-8 and colony formation results suggested that reducing SNRBP expression markedly reduced the cell proliferation of cervical cancer cells (Fig. 2B and C). The number and size of HeLa and SiHa spheres were obviously reduced when SNRBP was knocked down (Fig. 2D). By flow cytometry analysis,

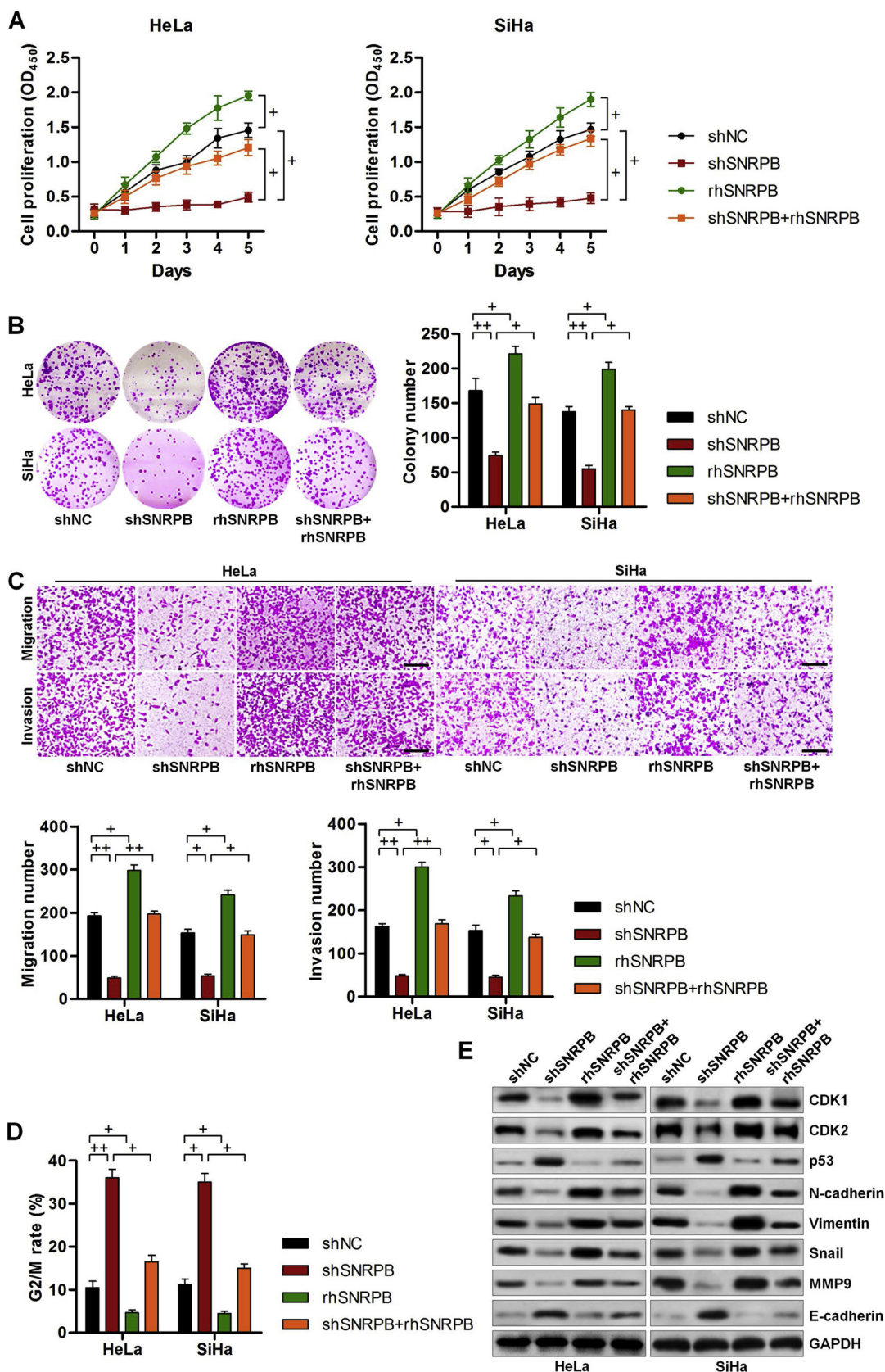


Fig. 4. Restoring SNRPB expression abolished shSNRPB-reduced proliferation, migration and invasion in breast cancer cells. (A–E) HeLa and SiHa cells were transfected with shSNRPB (#1) for 24 h, and then were incubated with or without 100 ng/ml of rhSNRPB for another 24 h. Then, all cells were harvested for the subsequent analysis. (A) Cell proliferation was measured using CCK-8 analysis. (B) Colony formation of cervical cancer cells treated as indicated. (C) Transwell analysis was used to determine the migration and invasion of cervical cancer cells. The number of cells in migration and invasion was quantified. (D) Flow cytometry analysis was used to calculate the number of cells distributed in the G2/M phase. (E) Western blotting analysis of CDK1, CDK2, p53, N-cadherin, Vimentin, Snail, MMP9 and E-cadherin in the treated cervical cancer cells. The data were presented as the mean ± S.E.M. *P < 0.05 and **P < 0.01.

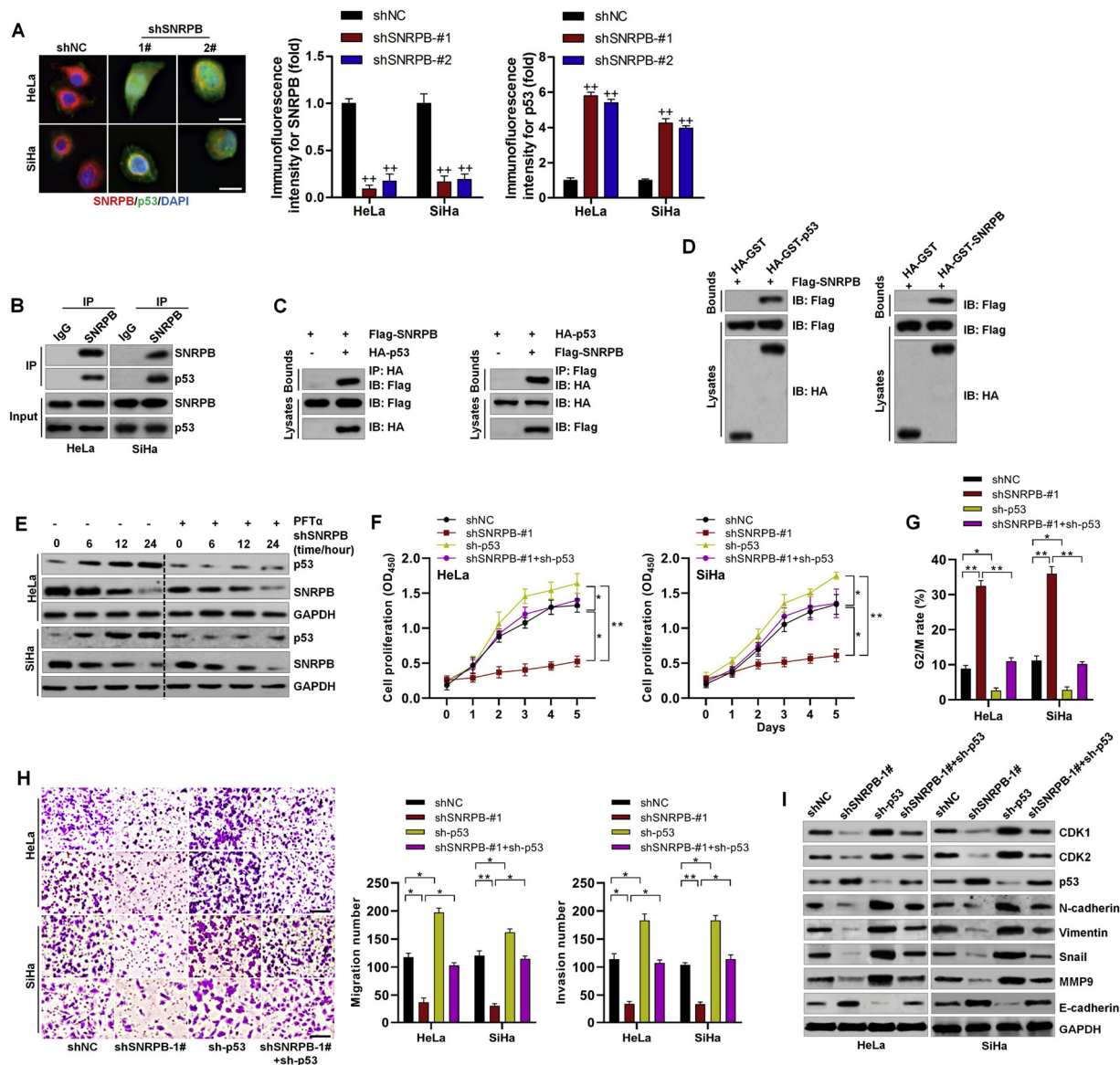


Fig. 5. SNRBP interacted with p53 and repressed its expression to modulate the progression of cervical cancer *in vitro*. (A) Immunofluorescence of SNRBP (red) and p53 (green) in cervical cancer cells with or without SNRBP knockdown. (B) HeLa and SiHa cells were treated with p53 activator of Tenovin-6 (10 μ M) for 24 h. Then, all cells were harvested for Co-immunoprecipitation analysis. (C) The co-IP assays in HeLa cells transfected with Flag-tagged SNRBP and HA-tagged p53. Anti-Flag and anti-HA antibodies were used as western blot probes. (D) GST precipitation assays showing direct SNRBP-p53 binding. Purified GST was used as a control. (E) HeLa and SiHa cells were transfected with or without shSNRBP for the indicated time, and then were treated with or without p53 inhibitor PFT α (10 μ M) for 6 h. Subsequently, all cells were collected for western blot analysis of p53 and Flag. (F–I) HeLa and SiHa cells were transfected with shSNRBP and/or sh-p53 for 24 h. Then, all cells were collected for the following analysis. (F) CCK8 analysis for cell proliferation. (G) Flow cytometry analysis for the evaluation of the percentage of cells in G2/M. (H) Transwell analysis for cell migration and invasion. (I) Western blotting results of signals related to cell cycle and metastasis. The data were presented as the mean \pm S.E.M. * P < 0.05 and ** P < 0.01.

we found that SNRBP decrease enhanced the percentage of cells in the G2/M phase when compared to the shNC group (Fig. 2E). Transwell analysis demonstrated that the number of migrated and invaded cervical cancer cells was significantly reduced by SNRBP knockdown (Fig. 2F–H). Meanwhile, the knockdown of SNRBP reduced the protein expression levels of cell cycle-associated signals CDK1 and CDK2, while elevated p53. Moreover, epithelial-to-mesenchymal transition (EMT) markers including N-cadherin, Vimentin, Snail and MMP9 were down-regulated in cervical cancer cells with SNRBP knockdown; however, E-cadherin expression levels were up-regulated (Fig. 2I). Together, results in this part elucidated that SNRBP was involved in the proliferation, migration and invasion processes that contributed to cervical cancer development.

3.3. SNRBP over-expression accelerated the proliferation, migration and invasion in cervical cancer cells

To confirm the effects of SNRBP on cervical cancer progression, we then over-expressed SNRBP in cervical cancer cells (Fig. 3A). CCK-8 assays demonstrated that SNRBP over-expression markedly promoted the proliferation of cervical cancer cells (Fig. 3B). The activity of SNRBP to promote the cell proliferation was confirmed by the colony formation assays (Fig. 3C). The number and size of HeLa and SiHa spheres were markedly enhanced when SNRBP was over-expressed (Fig. 3D). The transwell analysis demonstrated that SNRBP over-expression significantly enhanced the number of cells in migration and invasion (Fig. 3E). The percentage of cervical cancer cells distributed in G2/M was highly down-regulated when SNRBP was over-expressed by the

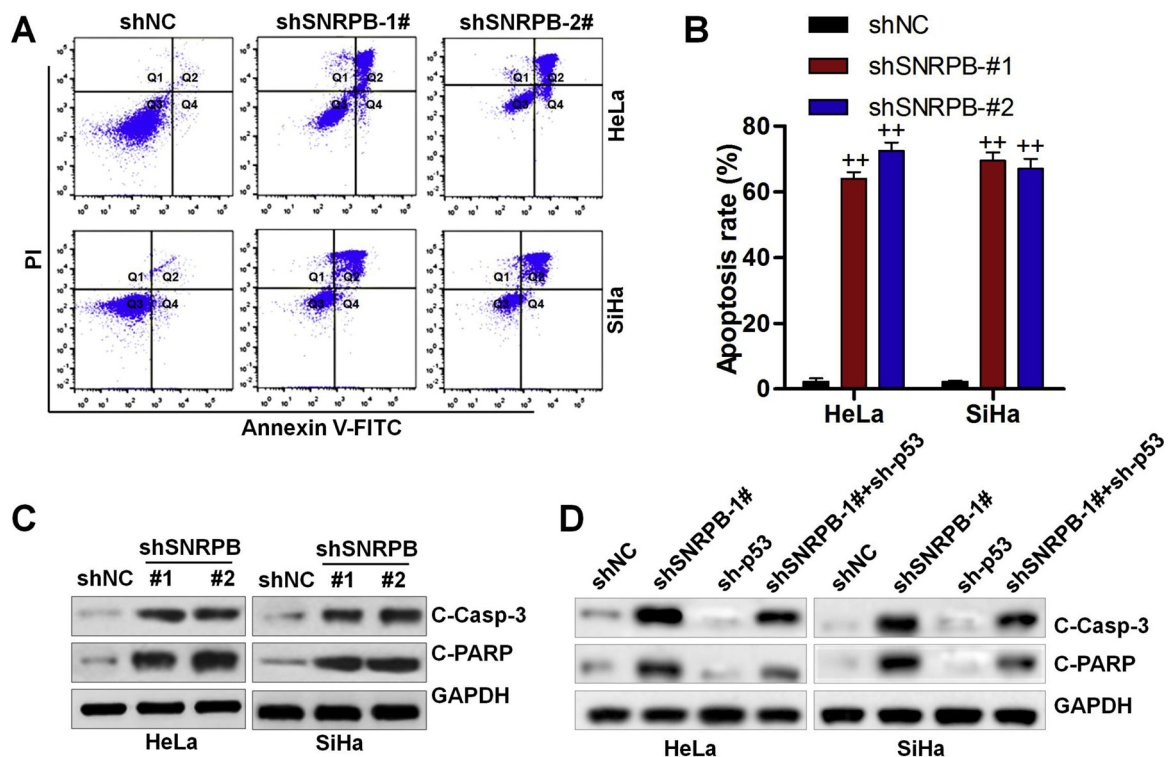


Fig. 6. Effects of SNRPB on apoptosis in cervical cancer cells. (A–C) HeLa and SiHa cells were transfected with shSNRPB-1# or shSNRPB-2# sequences for 24 h, and shNC was served as a control. (A,B) Apoptosis in cells was measured using flow cytometry analysis. (C) Western blot analysis for cleaved Caspase-3 and PARP in cells. (D) HeLa and SiHa cells were transfected with shSNRPB and/or sh-p53 for 24 h. Then, all cells were collected for the following analysis. Then, the cleaved Caspase-3 and PARP in cells were measured using western blotting analysis. The data were presented as the mean \pm S.E.M. ⁺P < 0.05 and ⁺⁺P < 0.01 compared to the shNC group.

flow cytometry analysis (Fig. 3F). Western blotting analysis showed that CDK1, CDK2, N-cadherin, Vimentin, Snail and MMP protein expression levels were up-regulated by SNRPB over-expression; however, p53 and E-cadherin expression levels were slightly reduced (Fig. 3G). These findings above demonstrated that SNRPB over-expression could promote cervical cancer progression by elevating the migration and invasion in cervical cancer cells.

To further confirm the effects of SNRPB on the progression of cervical cancer, we then rescued SNRPB expression in cells by the addition of rhSNRPB following its knockdown. As shown in Fig. 4A and B, CCK-8 and colony formation analysis demonstrated that SNRPB knockdown-reduced cell proliferation in cervical cancer cells was markedly restored by the treatment of rhSNRPB. Transwell analysis showed that the number of cervical cancer cells in migration and invasion was significantly reduced when SNRPB was knocked down compared to the shNC group. However, these effects were markedly rescued following rhSNRPB treatment (Fig. 4C). Moreover, we found that shSNRPB-increased the percentage of cells in G2/M phase was markedly abrogated by adding rhSNRPB in cervical cancer cells (Fig. 4D). Finally, western blotting analysis showed that the expression levels of CDK1, CDK2, N-cadherin, Vimentin, Snail and MMP9 were reduced by shSNRPB, while being again restored after rhSNRPB treatment; however, opposite results were observed in the expression change of p53 and E-cadherin (Fig. 4E). Taken together, these results demonstrated that rescuing SNRPB expression could recover the proliferation, migration and invasion of cervical cancer cells following its knockdown.

3.4. SNRPB interacted with p53 and repressed its expression to modulate the progression of cervical cancer in vitro

Increasing studies have reported that SNRPB plays a critical role in regulating cell proliferation and EMT process that are extremely

associated with tumor growth [9,10]. In this regard, immunofluorescence staining showed that SNRPB was apparently expressed in cervical cancer cells than that of p53, as evidenced by the stronger red fluorescence (referred to SNRPB) and weaker green fluorescence (referred to p53). In contrast, when SNRPB was knocked down, obviously increased p53 expression was detected in cervical cancer cells (evidenced by the stronger green fluorescence) (Fig. 5A). Furthermore, CO-IP analysis suggested that SNRPB interacted with p53 in cervical cancer cells (Fig. 5B). The Co-IP and GST pull-down assays confirmed that that SNRPB could directly interact with p53 (Fig. 5C and D). The p53 expression was decreased when its inhibitor PFT α was treated to cells with SNRPB knockdown (Fig. 5E). CCK-8 results then demonstrated that p53 knockdown markedly enhanced the cell proliferative ability in cervical cancer cells compared to the shNC group, and SNRPB knockdown-inhibited cell proliferation was, however, recovered almost to the shNC group by the knockdown of p53 (Fig. 5F). In addition, p53 knockdown significantly down-regulated the percentage of cells distributed in G2/M phase when SNRPB expression was repressed (Fig. 5G). Transwell analysis also showed that SNRPB knockdown-reduced the number of cervical cancer cells in migration and invasion was significantly reversed by p53 inhibition (Fig. 5H). Finally, western blot assays confirmed that CDK1, CDK2, N-cadherin, Vimentin, Snail and MMP9 protein expression levels suppressed by shSNRPB were apparently restored when cervical cancer cells transfected with sh-p53. By contrary, p53 and E-cadherin expression improved by SNRPB knockdown was evidently impeded when p53 was restrained (Fig. 5I). Together, findings above demonstrated that SNRPB knockdown-inhibited proliferation, migration and invasion in cervical cancer cells was closely dependent on p53 expression.

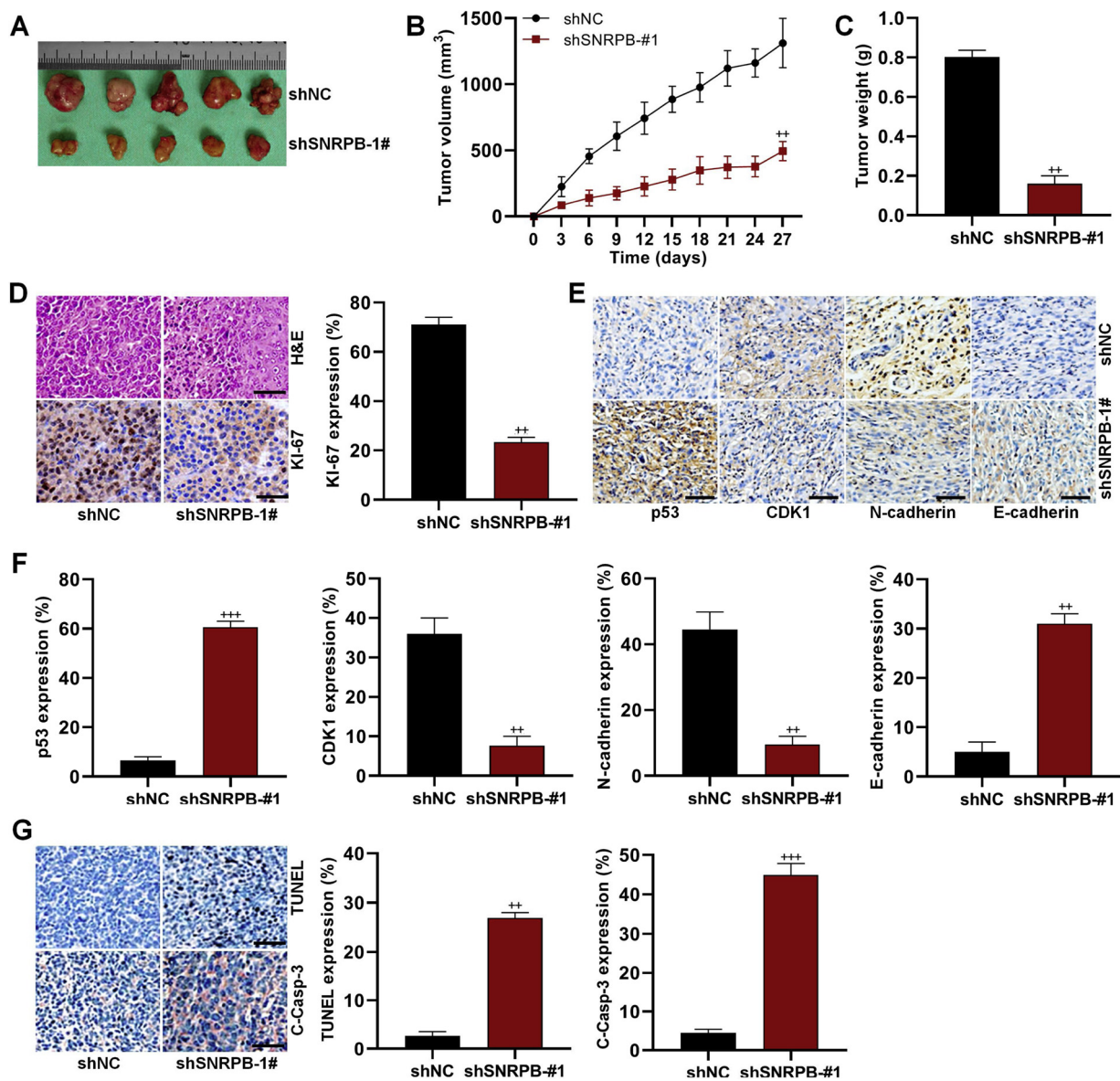


Fig. 7. Reducing SNRPB expression inhibited HeLa cell tumor growth *in vivo*. (A) Photos of tumor samples from mice. (B) Tumor volume was measured. (C) Tumor weight was calculated. (D) H&E staining and immunohistochemical analysis of KI-67 in tumor sections from mice. (E,F) Immunohistochemical analysis of p53, CDK1, N-cadherin and E-cadherin in tumor samples. The quantification of these signals was displayed. (G) Immunohistochemical analysis of TUNEL and cleaved Caspase-3 in tumor samples. The quantification of these signals was displayed. The data were presented as the mean \pm S.E.M. $^{**}P < 0.01$ and $^{***}P < 0.001$ compared to the shNC group.

3.5. Effects of SNRPB on apoptosis in cervical cancer cells

The effects of p53 on the regulation of apoptosis have been widely indicated [14,15]. Considering the direct relationship between SNRPB and p53, the role of SNRPB in mediating apoptosis was then investigated. Flow cytometry analysis demonstrated that SNRPB knockdown markedly induced apoptosis in cervical cancer cells (Fig. 6A and B). Meanwhile, the protein expression levels of cleaved Caspase-3 and PARP were up-regulated in cervical cancer cells when transfected with shSNRPB (Fig. 6C). Then, we also found that the cleaved Caspase-3 and PARP expression improved by SNRPB knockdown was evidently impeded when p53 was restrained (Fig. 6D). Thus, results in this regard demonstrated that reducing SNRPB expression could induce apoptotic cell death in cervical cancer, which was associated with p53 expression.

3.6. Reducing SNRPB expression inhibited HeLa cell tumor growth *in vivo*

HeLa xenografts models showed that SNRPB knockdown markedly reduced tumor growth and size compared to the shNC group, confirmed by the significantly decreased tumor volume and tumor weight (Fig. 7A–C). Tumor cell density and KI-67 expression levels were reduced in mice with SNRPB knockdown (Fig. 7D). As shown in Fig. 7E and F, immunohistochemistry validated that the knockdown of SNRPB obviously promoted p53 and E-cadherin expression levels in tumor sections, while CDK1 and N-cadherin expression was repressed consistent with the *in vitro* data. In addition, the number of TUNEL-positive cells was also up-regulated in tumor samples from mice with shSNRPB3, and consistent trend was detected in the expression change of cleaved Caspase-3 in tumor samples (Fig. 7G). These results confirmed that SNRPB knockdown showed anti-cervical cancer effects.

4. Discussion

Emerging evidences have suggested that SNRPB is highly expressed in different tumor tissues, and plays essential roles in regulating the progression of multiple tumors [9,10,16]. Accordingly, high expression of SNRPB was detected in glioma cell lines, and its deletion inhibited the cancer cell proliferation and enhanced the apoptosis [9]. In addition, the significantly increased expression of SNRPB was closely associated with poor prognosis of lung cancer [10,16]. Similar with previous studies, our findings showed that SNRPB exhibited an ectopic over-expression in cervical cancer tissues, and in multiple cervical cancer cell lines. Functional analysis revealed that SNRPB knockdown by shRNA significantly reduced the cervical cancer cell proliferative and colony formation capacity. Flow cytometry analysis indicated that SNRPB knockdown markedly induced the percentage of cells in the G2/M phase. The *in vitro* migrated and invaded abilities of cervical cancer cells were also blunted by SNRPB knockdown; however, these effects could be reversed when rhSNRPB was added to the cancer cells. Apoptosis in cervical cancer cells was also detected when SNRPB was knocked down through reducing the expression of cleaved Caspase-3 and PARP [17,18]. Importantly, we verified that SNRPB could directly interact with p53 by co-IP and GST pull down assays. SNRPB knockdown-induced G2/M phase, -triggered apoptosis and -inhibited migration and invasion of cervical cancer cells were extremely dependent on p53 expression. Our *in vivo* experiments confirmed the anti-cervical cancer effects of SNRPB knockdown by suppressing migration and invasion, and inducing apoptosis. All these mentioned findings illustrated that SNRPB exerted an oncogenic function during cervical cancer progression.

The abnormality of alternative splicing is defined as a key for tumor progression [19]. As reported, the alternative splicing of various genes is highly involved in the development of cervical cancer, and linked to the patient survival in cervical cancer [20]. SNRPB is demonstrated as a core component of spliceosome, which plays an essential role in mediating alternative splicing and then controlling gene expression [6,7,21]. Recently, SNRPB was shown to be over-expressed in different tumor tissues such as glioma, breast cancer and lung cancer [9,10,16]. For instance, highly decreased SNRPB expression contributed to the migration and invasion of NSCLC cells based on the *in vitro* and *in vivo* experiments [10]. However, SNRPB was also identified as a suppressor for metastasis in an animal allograft model of prostate cancer [22]. These findings suggest that SNRPB may have different roles if modulating tumor genesis dependent on context. Here, in this current study, we found that SNRPB knockdown markedly reduced the migration and invasion of cervical cancer cells, which was also evidenced by the apparently reduced expression of N-cadherin, Vimentin, Snail and MMP9. These signals play an important role in facilitating EMT, a critical program for the invasion and metastasis [23,24]. E-cadherin is also a hallmark of EMT, and its up-regulation contributes to the suppression of EMT process [25]. Here, we also found that SNRPB knockdown markedly improved E-cadherin expression, indicating the suppression of migration and invasion.

Cell cycle de-regulation leading to the uncontrolled cell proliferation is one of the most frequent alterations that occur during cervical cancer progression [26]. The G2/M checkpoint plays an essential role in maintaining chromosomal integrity through allowing cells to repair DNA damage before entering mitosis. CDK1 and CDK2 are two crucial mediators for the cell cycle at G2/M checkpoint [27,28]. In this work, we demonstrated that SNRPB decrease-inhibited cell proliferation was partly attributed to the decreases in CDK1 and CDK2 expression. Increasing studies have showed that p53, a well-known tumor suppressor, is tightly associated with the progression of cell cycle, and induces G2/M arrest in various types of tumors, including cervical cancer [29,30]. Meanwhile, mutant p53 could drive migration and invasion in cervical cancer *via* different signaling pathways [31,32]. In our present study, we also found that p53 expression was induced by the knockdown of

SNRPB. CO-IP assays demonstrated that SNRPB could interact with p53 in cervical cancer cells. The *in vitro* analysis showed that shSNRPB-reduced cell viability, migration and invasion, and -induced G2/M arrest were significantly reversed by p53 knockdown. Therefore, we enriched the regulatory effects of SNRPB on tumor growth, and p53 might be a new target through which SNRPB knockdown displayed anti-cervical cancer ability. However, we could not exclude that SNRPB might be also involved in the progression of other types of cancers due to its higher expression levels in gastric cancer, breast cancer and lung cancer. As for this, further studies are still warranted in future to comprehensively demonstrate the molecular mechanisms by which SNRPB regulates the development of cervical cancer or even other types of tumors.

In conclusion, our findings indicated that SNRPB was a clinical marker for cervical cancer. Additionally, SNRPB down-regulation could inhibit cervical cancer cell proliferation, migration and invasion, while improves cell cycle arrest in G2/M. These processes were mainly through its interaction with p53. Thus, it may be fruitful to develop SNRPB-selective inhibitor for cervical cancer treatment.

Declaration of Competing Interest

The authors declared that they have no conflicts of interest to this work.

Appendix A. Supplementary data

Supplementary material related to this article can be found, in the online version, at doi:<https://doi.org/10.1016/j.biopha.2020.109948>.

References

- [1] E.J. Crosbie, M.H. Einstein, S. Franceschi, et al., Human papillomavirus and cervical cancer, *Lancet* 382 (9895) (2013) 889–899.
- [2] S. de Sanjose, W.G.V. Quint, L. Alemany, et al., Human papillomavirus genotype attribution in invasive cervical cancer: a retrospective cross-sectional worldwide study, *Lancet Oncol.* 11 (11) (2010) 1048–1056.
- [3] X. Hu, J.K. Schwarz, J.S. Lewis, et al., A microRNA expression signature for cervical cancer prognosis, *Cancer Res.* 70 (4) (2010) 1441–1448.
- [4] S. Stevanović, L.M. Draper, M.M. Langhan, et al., Complete regression of metastatic cervical cancer after treatment with human papillomavirus-targeted tumor-infiltrating T cells, *J. Clin. Oncol.* 33 (14) (2015) 1543.
- [5] L. Denny, Cervical cancer: prevention and treatment, *Discov. Med.* 14 (75) (2012) 125–131.
- [6] T.A. Gray, M.J. Smithwick, M.A. Schaldach, et al., Concerted regulation and molecular evolution of the duplicated SNRPB/B and SNRPN loci, *Nucleic Acids Res.* 27 (23) (1999) 4577–4584.
- [7] S. Bacrot, M. Doyard, C. Huber, et al., Mutations in SNRPB, encoding components of the core splicing machinery, cause cerebro-costo-mandibular syndrome, *Hum. Mutat.* 36 (2) (2015) 187–190.
- [8] M. Tooley, D. Lynch, F. Bernier, et al., Cerebro-costo-mandibular syndrome: clinical, radiological, and genetic findings, *Am. J. Med. Genet. A* 170 (5) (2016) 1115–1126.
- [9] B.R. Correa, P.R. de Araujo, M. Qiao, et al., Functional genomics analyses of RNA-binding proteins reveal the splicing regulator SNRPB as an oncogenic candidate in glioblastoma, *Genome Biol.* 17 (1) (2016) 125.
- [10] N. Liu, Z. Wu, A. Chen, et al., SNRPB promotes the tumorigenic potential of NSCLC in part by regulating RAB26, *Cell Death Dis.* 10 (9) (2019) 1–11.
- [11] X. Li, J. Jin, S. Yang, et al., GATA3 acetylation at K119 by CBP inhibits cell migration and invasion in lung adenocarcinoma, *Biochem. Biophys. Res. Commun.* 497 (2) (2018) 633–638.
- [12] J. Wu, J. Choiniere, M. Lin, et al., Pyruvate dehydrogenase kinase 4-deficiency induces hepatic apoptosis by activating NF- κ B/TNF α signaling, *FASEB J.* 31 (1_Suppl) (2017) 470.9.
- [13] C. Zhang, J. Lei, P. Yu, et al., Walsurionid B induces mitochondrial and lysosomal dysfunction leading to apoptotic rather than autophagic cell death via ROS/p53 signaling pathways in liver cancer, *Biochem. Pharmacol.* 142 (2017) 71–86.
- [14] N. Thorenor, P. Faltejskova-Vychytilova, S. Hombach, et al., Long non-coding RNA ZFAS1 interacts with CDK1 and is involved in p53-dependent cell cycle control and apoptosis in colorectal cancer, *Oncotarget* 7 (1) (2016) 622.
- [15] M. Ye, J. Zhang, J. Zhang, et al., Curcumin promotes apoptosis by activating the p53-miR-192-5p/215-XIAP pathway in non-small cell lung cancer, *Cancer Lett.* 357 (1) (2015) 196–205.
- [16] I. Valles, M.J. Pajares, V. Segura, et al., Identification of novel deregulated RNA metabolism-related genes in non-small cell lung cancer, *PLoS One* 7 (8) (2012) e42086.
- [17] J. Baharara, T. Ramezani, A. Divsalar, et al., Induction of apoptosis by green

- synthesized gold nanoparticles through activation of caspase-3 and 9 in human cervical cancer cells, *Avicenna J. Med. Biotechnol.* 8 (2) (2016) 75.
- [18] L.R. Nath, J.N. Gorantla, S.M. Joseph, et al., Kaempferide, the most active among the four flavonoids isolated and characterized from *Chromolaena odorata*, induces apoptosis in cervical cancer cells while being pharmacologically safe, *RSC Adv.* 5 (122) (2015) 100912–100922.
- [19] S. Alsafadi, A. Houy, A. Battistella, et al., Cancer-associated SF3B1 mutations affect alternative splicing by promoting alternative branchpoint usage, *Nat. Commun.* 7 (2016) 10615.
- [20] E.J. Lee, M. Jo, J. Park, et al., Alternative splicing variants of IRF-1 lacking exons 7, 8, and 9 in cervical cancer, *Biochem. Biophys. Res. Commun.* 347 (4) (2006) 882–888.
- [21] Y.L. Tay, Mutations within the spliceosomal gene SNRPB affect its auto-regulation and are causative for classic cerebro-costo-mandibular syndrome, *Clin. Genet.* 1 (87) (2014) 32–33.
- [22] Y. Yi, S. Nandana, T. Case, et al., Candidate metastasis suppressor genes uncovered by array comparative genomic hybridization in a mouse allograft model of prostate cancer, *Mol. Cytogenet.* 2 (1) (2009) 18.
- [23] M. Rokavec, M.G. Öner, H. Li, et al., IL-6R/STAT3/miR-34a feedback loop promotes EMT-mediated colorectal cancer invasion and metastasis, *J. Clin. Invest.* 124 (4) (2014) 1853–1867.
- [24] R. Qureshi, H. Arora, M.A. Rizvi, EMT in cervical cancer: its role in tumour progression and response to therapy, *Cancer Lett.* 356 (2) (2015) 321–331.
- [25] Y. Cheng, Y. Zhou, W. Jiang, et al., Significance of E-cadherin, β -catenin, and vimentin expression as postoperative prognosis indicators in cervical squamous cell carcinoma, *Hum. Pathol.* 43 (8) (2012) 1213–1220.
- [26] M. Naemura, C. Murasaki, Y. Inoue, et al., Long noncoding RNA ANRIL regulates proliferation of non-small cell lung cancer and cervical cancer cells, *Anticancer Res.* 35 (10) (2015) 5377–5382.
- [27] B. Lohberger, A. Leithner, N. Stüendl, et al., Diacerein retards cell growth of chondrosarcoma cells at the G2/M cell cycle checkpoint via cyclin B1/CDK1 and CDK2 downregulation, *BMC Cancer* 15 (1) (2015) 891.
- [28] V. Oakes, W. Wang, B. Harrington, et al., Cyclin A/Cdk2 regulates Cdh1 and claspin during late S/G2 phase of the cell cycle, *Cell Cycle* 13 (20) (2014) 3302–3311.
- [29] Z. Zhang, C.Z. Wang, G.J. Du, et al., Genistein induces G2/M cell cycle arrest and apoptosis via ATM/p53-dependent pathway in human colon cancer cells, *Int. J. Oncol.* 43 (1) (2013) 289–296.
- [30] G. Yao, M. Qi, X. Ji, et al., ATM-p53 pathway causes G2/M arrest, but represses apoptosis in pseudolaric acid B-treated HeLa cells, *Arch. Biochem. Biophys.* 558 (2014) 51–60.
- [31] C.L.A. Yeung, T.Y. Tsang, P.L. Yau, et al., Human papillomavirus type 16 E6 induces cervical cancer cell migration through the p53/microRNA-23b/urokinase-type plasminogen activator pathway, *Oncogene* 30 (21) (2011) 2401.
- [32] M. Shi, L. Du, D. Liu, et al., Glucocorticoid regulation of a novel HPV-E6-p53-miR-145 pathway modulates invasion and therapy resistance of cervical cancer cells, *J. Pathol.* 228 (2) (2012) 148–157.